Rotationally invariant statistics for examining the evidence from the pores in fingerprints.

N.R. Parsons[*], J.Q. Smith[†], E. Thönnes[‡]
Department of Statistics, University of Warwick, Coventry, CV4 7AL, UK

L. Wang[§] and R.G. Wilson[¶]
Department of Computer Science, University of Warwick, Coventry, CV4 7AL, UK

Abstract

Recent methodological advances in the processing of DNA evidence have begun to force a closer examination of assertions about the strength of other sorts of evidence. One traditional source of evidence is the fingerprint. Currently a print taken from a suspect is compared against a mark from a crime scene and a match declared using the judgement of an expert based on matching minutiae and the ridge patterns around these. However such methods have proved difficult to quantify effectively. This has provoked the investigation of even finer features in the print and the mark. One set of such features are the many pores, located along the ridges of the fingerprint. Is it possible to supplement expert judgements associated with a match with a more automatic and quantitative measure of the strength of evidence, based on pore information? The results of this preliminary analysis suggests we can. Our methodology is relatively transparent, using common statistics for two sample comparisons of point patterns. The results discussed here concern the matching of inked prints using grey level imaging and complement previous studies which tend to focus on the comparison of binarised images.

[*]n.parsons.1@warwick.ac.uk
[†]J.Q.Smith@warwick.ac.uk
[‡]Corresponding author: E.Thonnes@warwick.ac.uk
[§]Li.Wang@warwick.ac.uk
[¶]Roland.Wilson@warwick.ac.uk

Keywords: Fingerprints, Level 3 features, pore pattern, pore extraction, non-parametric spatial statistics.

1 Introduction

With the advent of the use of systematic and well supported methodologies for the analysis of the strength of DNA evidence, there has been increasing pressure to produce analogous methodologies for use with other forms of evidence; especially fingerprint evidence. An important development was the use of a point rule for declaring an identification based on the comparison between a print taken from a suspect and a mark retrieved from the crime scene. An expert examined the two images for singularities in the ridge pattern, called *minutiae*, such as ridge endings, bifurcations, etc. Based on rather contentious statistical assumptions about the randomness of configurations of minutiae, the rule then declared a match between the print and the mark if a fixed number (16 in the UK) of matching minutiae were found. However this methodology has since been largely abandoned. This was not only because the foundations of this inferential framework have been criticised: the independence assumptions and particularly the way that common and uncommon minutiae are treated exchangeably [2, 4]. Also the severity of the criterion made it difficult to apply routinely. However current methods for matching fingerprints replacing these methods, such as those used by NAFIS, still rely exclusively on the identification of minutiae [3, 7].

In this paper we suggest a different way of comparing a print to a mark which may supplement or replace the use of minutiae. On both the mark and the print there is a set of pore marks [3], the light spots which can be seen in the centres of the ridges in a typical fingerprint image, such as Figure 1.

We know that these pores are often used heuristically by experts to supplement minutiae information and help them come to a judgement about whether or not the mark and print match. But is it possible to use the pore configurations on the mark and the print formally to enhance our confidence that the mark came from the suspect?

Already serious advances in understanding the nature of pores in their use as identification evidence have been made see for example [1, 3, 12, 13, 14]. Most current methods begin with a grey level extraction algorithm but then proceed immediately to a binarised image: i.e. an image where all pixels are coloured either white or black. The binarised images of the mark and print are then compared. For example in [12], pores are studied as a tool to authenticate people using live-scan prints. However, often pores are treated as if they are amenable to the same type of analysis as minutiae. Various alterna-

Figure 1: A typical fingerprint image; only the central section is shown.

tive match statistics are then used which simply count various proportions of "feature matches" within segments of the image. The definition of a "match" appears to us rather arbitrary and often historical: sometimes chosen because they were an obvious choice in now discredited models of independence. Finally, probabilities are assigned to the values of these statistics using sample proportions which then allow the computation of "theoretical" false positive and false negative classification characteristics of different algorithms. However, such an approach appears to us as using rather dubious independence assumptions: see for example in [12] the criticism of the Ashbaugh model [1].

In practice, a suspect's print would need to be matched against a mark left at the scene of the crime. In this study we contented ourselves with comparing inked prints with other inked prints. This would give an upper bound to the extent to which a print and a mark from the same finger could be matched. The data was kindly provided to us by the Police Science Development Branch and consisted of 256×256 pixel images of 108 inked prints at a resolution of 1000 dpi (dots per inch). In a first experiment four separate prints from each of four fingers from three male individuals were taken, yielding 48 prints. In a second experiment for each of five different pressures six separate prints of two fingers from a female individual were taken.

Instead of using a binarised image to extract pores as in [14] we chose a relatively sophisticated method of grey level extraction based on a principal components analysis [8] of a large class of putative pores. This algorithm is

briefly discussed in Section 2, further details are given in Appendix A.

In Section 3 we describe how this output can be analysed using standard statistical summaries associated with a paired comparison of two point processes. Our methodology ignores the ridge structure after the identification of pores and concentrates on comparing the scatter of pore locations in the two images. We note that some authors cited above have recommended ignoring ridge information under certain conditions of the mark. Moreover, choosing to ignore explicit ridge structure did not appear too radical since it was usually possible to see where most of the ridges went by examining the pore locations alone. In fact an automatic method for inferring the ridge structure from a given pore pattern is currently under development.

A match between prints can now be defined in terms of these standard spatial statistics whose properties are well understood, see e.g. [5]. While we illustrate how these standard statistics appear to give very strong discriminatory power, our aim here is to underline the evidential value of fingerprints rather than give a specific criterion for declaring a match between two prints.

Pressure had long been recognised as an important determinant of the image. Our techniques also allow us to compare inked prints of the same finger at different pressures. This enabled the study to address the possible corruption arising from the (uncontrolled) pressure made by the perpetrator when he left a mark at a scene of crime.

We note that the results reported here are indicative rather than definitive since they are not based on the appropriately designed population sample which is envisaged for the future. Our results summarise a detailed analysis of the prints from a relatively small number of individuals. However we believe that these results are promising enough to encourage further investigation. In the last section we examine various ways forward.

2 Grey level modelling and PCA

When comparing two fingerprints using an automatic procedure they need to be mutually aligned. This is a complex task as distortions, for example due to the plasticity of the finger, are non-linear. Such methods are commonly based on the large scale characteristics of the two prints. The alignment is then usually performed through the translation and rotation of one of the images. We used a rigid alignment model, a simplified version of the alignment procedure described in [6]. The appropriate rotation and translation were determined based on the Fourier spectra of the two images. The magnitude spectrum was used to estimate the rotation, following which, the cross-correlation of the rotated images was used to estimate the translation.

Henceforth in this paper we assume that this alignment, called registration, has been performed.

Our pore extraction algorithm began by using a simple thresholding operation on the bandpass filtered 256×256 pixel image. Bandpass filters have been used previously in this context see e.g. [12, 13, 14], but often only on the way to constructing a binarised image. Binarised images are not ideal for the comparison of pore configurations. The segmentation of the image into a cellular structure loses its rotational symmetry, the elaboration of models to include covariates is non-trivial and any realistic distribution of a "match" not only for prints of the same finger but also for images of different fingers is difficult to calculate and defend. Furthermore the naive use of grey level filters to construct the binarised image in the papers cited above was coarse and led to difficult decisions about the balancing of false rejections and acceptances. (For recent notable exception of a feature extraction algorithm that does not rely on binarisation see for example [10].)

We used a grey level filter to identify those areas of the image containing *any* feature which might be a pore (henceforth called a *putative pore*): aiming for a zero false rejection rate. One obvious characteristic of a pore feature is that it is usually more or less circular in shape and brighter than the surrounding ridge structures.

This extraction phase was followed by a sieving phase, in which the grey level distribution in a window surrounding the nominal centres (centroids) of the putative pores was modelled using a principal component analysis (PCA) [8]. This allowed us to reject those features which deviated significantly from the average pore shape, whilst allowing for a degree of variability found in typical fingerprint images. We found that the appropriate settings threshold parameters, needed for performing this sieving, were fairly robust across different individuals and images.

Our algorithm therefore formally extracted the location on a print of 'averagely shaped' pore-like features: not necessarily containing some of the rather irregularly shaped features that an expert might be able to recognise as the biological reality of a sweat gland. This re-definition enabled us to extract a formally defined collection of features without reference to expert judgement. These could then be compared with another collection of automatically extracted features. When comparing the output of one specific print with the configurations of pores extracted by an expert, the error rate from this procedure was found to be about 30%. The error included both extracted features that had not been identified by the expert and pores identified by the expert but not extracted by our algorithm. However, considering that our definition of a pore was rather different from the one used by the expert, this appeared a good enough match for us to be able to reasonably

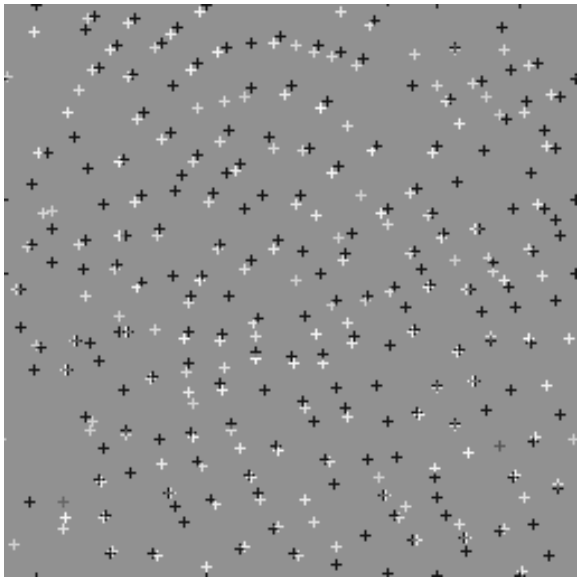

Figure 2: The figure above shows two sets of pores extracted from two different prints of the same finger registered to one another. White crosses show the pore locations of the first print, black crosses the pores of the second print. Grey crosses indicate pore locations that coincide in both prints.

refer to our extracted features as "pores".

Figure 2 shows the estimated centroids of the putative pores for two different prints of the same finger after alignment. Because of the plasticity of the finger, even on high quality prints, two replicate images of the same finger were inevitably different: the collections of pores each being displaced slightly differently from image to image. Thus we could not expect pores on two images of the same finger to match precisely, even after the images had been orientated appropriately.

We now focus on comparing the statistical properties of configurations of matching pores when two prints were taken from the same finger against their properties when taken from different fingers.

3 Some Simple Spatial Statistics

From a statistical perspective, the centroids of pores are *events* in a point process. Established statistical methods for analysing point patterns are available as packages, such as "Splancs" or "spatstat", in the free statistical computing environment "R" [11].

Statistical methods for spatial point processes often involve comparisons between empirical summary descriptions of their respective patterns. In this paper we report results associated with the two-sample versions of just two such statistics which give useful insights into the first and second order properties of the given patterns of events. Commonly these summary statistics are based on distances between the events. The configuration of pore centroids are usually non-homogeneous and form directional patterns. They are therefore not stationary or isotropic: assumptions that are common for analyses of point processes. However paired comparisons require much less stringent conditions.

In a later paper we will report how the distribution of the two sample statistics of two images of the same finger discussed in this paper can be derived as a mixture of an approximate isotropic process and a contaminating process which is approximately locally isotropic. The distribution of statistics of two different fingers is more difficult. It is dependent on the initial orientation of the two images and cannot be calculated theoretically except through reference to survey information, currently unavailable, about the closeness of pore configurations across the population. If likelihood ratio methods are used, then this information will be required. However, on the basis of a detailed examination of the images in our sample space, we are reasonably confident that such a survey will demonstrate robust characteristics, often giving rise to distributions of the statistics close to those expected when comparing two Poisson (random) point pattern. In a Poisson point pattern the number of points follows a Poisson distribution and the locations of points are independent and identically distributed uniformly on the sampling window. Numerical methods [5] are conventionally used to analyse spatial point processes and these can legitimately be used in this context.

3.1 Bivariate nearest neighbour distance distribution function

To compare realisations of two point processes it is natural to consider the relationship between a typical event in the first point pattern and the nearest neighbouring event in the second pattern. When comparing fingerprints for use in criminal trials, the first point pattern will be the pores from the crime scene and the second the pores in the inked print taken from the suspect. As we have previously stated, in our study the mark will be substituted by a second print from our database. Despite two prints of the same finger never corresponding precisely we might reasonably expect many more closely located events than if the prints came from different fingers. This can be

examined more formally as follows.

Consider the distribution function G_{12} of the distance between a typical pore in the first print and nearest pore in the second print. This distribution function can be estimated from the data and is commonly known as the nearest-neighbour distribution function. An explicit definition of its estimator $\widehat{G}_{12}$ and related statistics can be found in Appendix B. Similarly, we can also estimate the probability density function g_{12} associated with G_{12}. Figure 3 displays an estimate of g_{12} in (a) and G_{12} in (b). Note how the histogram in Figure 3 (a) exhibits a "shoulder" on the right. This was discovered to be a feature when comparing different prints from the same finger.

Figure 4 (a) and (b) below show estimates of G_{12} and g_{12} when comparing two prints from different fingers. The mode of the histogram in Figure 4 (a) lies to the right of the mode of the histogram in Figure 3 (a). Similarly, the distribution function in 3 (b) shows a steeper incline than the one in 4 (b). This is consistent with the expectation that for prints from different fingers nearest pores will lie further apart than for prints from the same finger.

Whilst calibrating the pore extraction algorithm we had noticed that our experts tended to declare a match between two pores on different images if and only if they were less than about 10 pixels apart. This, and the shoulder apparent in estimates of g_{12} for prints of the same finger, suggested that the distributions above were mixtures of well matched and spuriously matched pores. Here the 10 pixel threshold acted as a kind of crude discriminant. Figures 3 (c) and 4 (c) show histograms of the nearest pore distances of less than ten pixels. These correspond to pores that would have been considered for matching by the expert. The two histograms look markedly different and so provide promising summaries that may enable us to differentiate whether two prints come from the same finger or from different fingers. In contrast to the previous histograms, the histograms for nearest pore distances greater than ten pixels are very similar whether the prints came from the same finger or from different fingers. This suggests that these distances correspond to spurious matches of pores.

It is helpful to plot the deviation of G_{12} from what we might expect when comparing two random patterns. Assume we have two independent realisations of the same Poisson point process, that is the number of points in each realisation is Poisson distributed with the same mean and the locations of points are independent and uniformly distributed on the sampling window. In this case the nearest neighbour distribution function G_{12} is known explictly and given in Appendix B. We call it F_2 to distinguish it from the nearest neighbour function derived from the comparison between two pore patterns.

Figure 5 displays $\widehat{G}_{12} - F_2$ for prints of the same finger and of different fingers. For prints of the same finger we find that the distances between

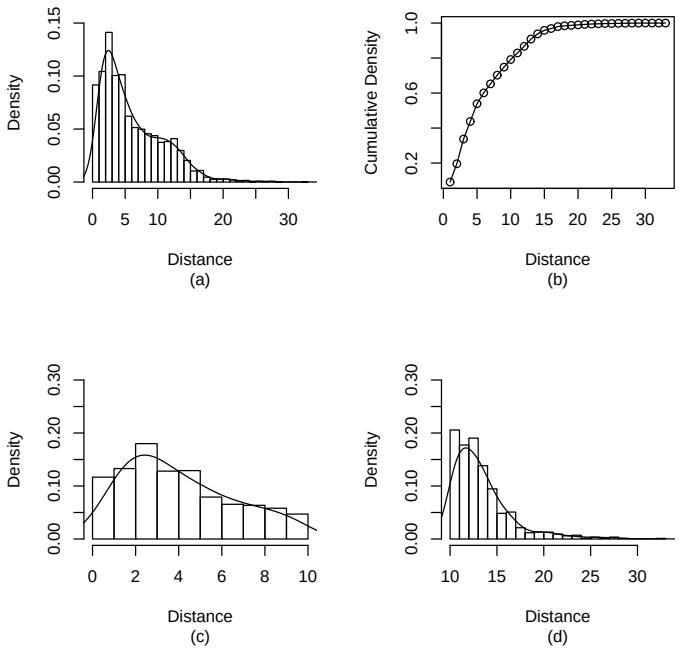

Figure 3: Distribution of distances between nearest pores in two prints of the same finger: (a) the density estimate, (b) the estimate for the cumulative distribution function (cdf), (c) a histogram of the distances less than ten pixels and (d) of distances greater than or equal to ten pixels.

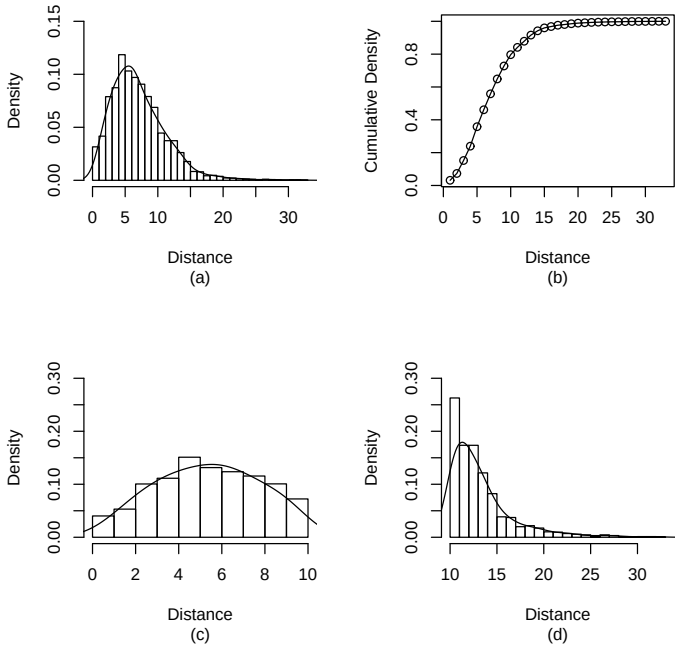

Figure 4: Distribution of nearest pore distances in two prints of different fingers: (a) the density estimate, (b) the estimate for the cdf, (c) histogram of the distances less than ten pixels and (d) of distances greater than or equal to ten pixels.

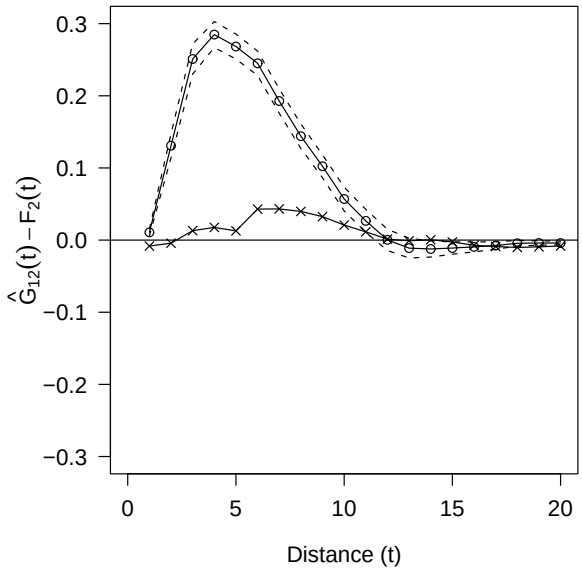

Figure 5: $\widehat{G}_{12}(t) - F_2(t)$ for two prints of the same finger (o) (shown with two bootstrap standard error limits) and $\widehat{G}_{12}(t) - F_2(t)$ for two prints of different fingers ($\times$).

matched pores are typically much smaller than what we expect from two independent, random patterns. In contrast, for two prints of different fingers (but with similar ridge structure) the estimate $\widehat{G}_{12}$ is very similar to F_2. We note again the clear difference in the automatic outputs between same finger and different finger comparisons. This was a common feature in *all* analogous comparisons of images in our database strongly suggesting that this differentiation is ubiquitous.

With the same caveats we made before about the appropriateness of the quoted probability thresholds these summary functions therefore promise to determine with a high degree of certainty whether the pore patterns originated from the same or different fingers.

3.2 Ripley's K-function

A second, routinely calculated descriptive statistic of the second-order properties of point processes is Ripley's K-function. The bi-variate version K_{12} allows a comparison between two point processes. Here $K_{12}(t)$ is the expected proportion of events in the second point pattern that lie within a circle of radius t centred at a typical event in the first pattern. This can be estimated from the number of pores in the second print that lie within distance t from

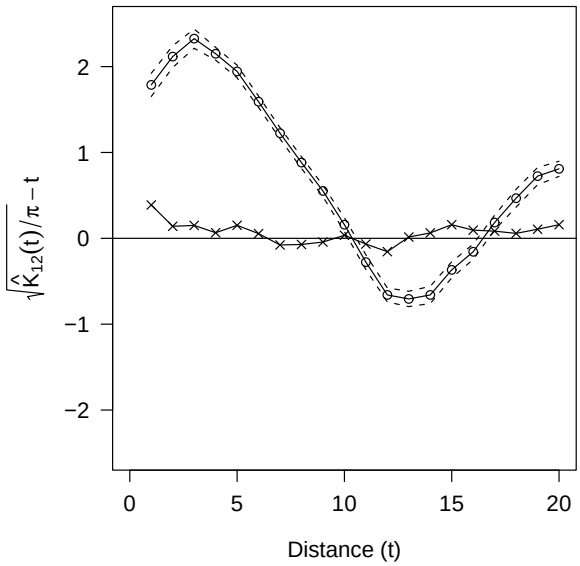

Figure 6: $\sqrt{\widehat{K}_{12}(t)/\pi} - t$ for two prints of the same finger (o) (shown with two bootstrap standard error limits) and $\sqrt{\widehat{K}_{12}(t)/\pi} - t$ for two prints of different fingers $\times$.

a pore in the first print, see Appendix B for more details. We can reasonably expect that a print compared to another print from the same finger would have smaller interpore distances than when compared to a print from a different finger. Thus for small t we expect $K_{12}(t)$ to be larger in the first case than in the second. If the two stationary point processes are independent, then $K_{12}(t) = \pi t^2$. This will not be so in this example. However it again provides us with a useful benchmark for this statistic.

In order to stabilise the variance and to linearize plots under the independence assumption, in Figure 6 we plotted $\sqrt{\widehat{K}_{12}(t)/\pi} - t$ when comparing prints of the same finger, and prints of different fingers. Without making erroneous assumptions [5] we can use our data set to produce bootstrap bounds for pairs of prints of the same finger. These are also given in Figure 6. The shapes of these graphs for prints of the same finger and prints of different fingers were strongly consistent over all prints we had available to us. One interesting feature of $K_{12}(t)$ for prints of different fingers is the similarity of the plot to that expected under the independence assumption.

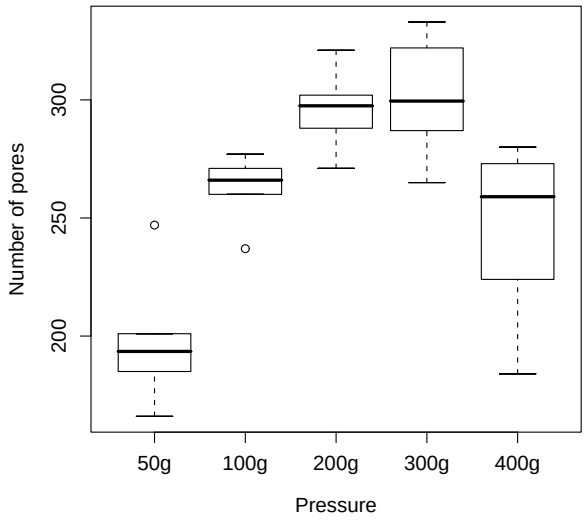

Figure 7: Boxplot of pore counts for prints of the same finger taken at 50g, 100g, 200g, 300g and 400g pressure.

3.3 Between-subjects comparison of Pressure Depletion

Using bootstrap methods it was also possible to examine the effects of various covariates on the matching characteristics for two prints of the same finger. We conclude by demonstrating this type of analysis on the effects of numbers of retained pores.

Figure 7 shows a Boxplot of pore counts for six replicates of fingerprints obtained at pressures of 50g, 100g, 200g, 300g and 400g for one of our subjects. While there was some measurable difference in the number of pores successfully identified on the inked prints, provided that the pressures applied were not extremely light, this effect was not dramatic.

This meant that the plots of the statistics discussed in the previous sections were similar to the ones associated with a standard pressure except for the the extremely light 50g pressure. We therefore conjecture that for light pressures these statistics may not be discriminating. However, given a minimum pressure was applied, the statistics appeared to be discriminating under varying pressures. This is an important property to exhibit because in practice there would be no control on the pressure of the mark retrieved from the scene of crime.

4 Conclusions

These initial indications suggest that an analysis based simply on configurations of centroids of pores appears to work quite well even under linear re-alignment. As many authors have demonstrated (see e.g. [12]) independence assumptions used to assess the evidential value of pore configurations in a given print are not appropriate in practice and are clearly violated. However the distributions of *certain statistics* associated with the difference between the pore pattern of two individuals appeared surprisingly close to the distributions of the same statistics for two point patterns that are random and independent: at least over the small number of individuals we observed in this study. Furthermore, depending on the registration algorithm of images, the pore alone statistics reported here appear to have a distribution not strongly dependent on statistics that count, identify and position other minutiae information that might be present in the print and mark. If these properties could be confirmed on a large sample survey then the strength of evidence given by a statistic for and against the hypothesis that the pore configuration came from the same finger could be calculated simply and explicitly.

We have recently shown that there is useful information in the further characteristics of the pore events: that is, useful information in the size and shape of pores. This information appears potentially very useful for providing registration information, both for pore configurations themselves when other information such as that from minutiae is weak, and also to calibrate important covariates associated with the mark, such as the pressure used in making the mark, and so obtain better match characteristics.

Of course, all these comments are based on the caveat that a large properly designed balanced survey is now needed to confirm these conjectures. Here this could be used specifically to determine the actual distribution of statistics on pore configurations both within the same finger and across different fingers, for the population as a whole, indexed by important covariates. It appears to us that such a study could easily be anonymised as they might be from statistics associated with medical records and should therefore be implementable. On the basis of such information, statements like,"We would only expect a match between these two pore configurations one time in 10^6 were the images actually from two different fingers whilst this quality or worse would be obtained 99% of the time if from the same finger." In contrast, due to the complexity of the underlying pore generating process, arguments based on combinatorics on assumed independence assumptions appear fragile, sensitive to certain model assumptions and potentially open to misinterpretation unless extreme care is taken.

Finally we found, as had been previously suspected by our experts, that heavily degraded images of pores contain little evidential value. It is less clear whether good quality marks on small regions would not provide strong enough evidence. Therefore it is probably wise to focus any future study on matching prints to (possibly small but) good quality marks. However, due to contamination and inherent dependence, matching on 20 pores as has been previously suggested [1] appears to us overly optimistic. On the basis of this study we would conjecture that good marks with more than about 80 pores appear to have potentially strong evidential value using this extraction algorithm.

Appendix A The pore extraction algorithm

To detect circular features the algorithm uses the difference of Gaussian (DOG) filter [9]

$$l(x,y) = \exp[-0.5(x^2+y^2)] - \frac{1}{2}\exp[-0.25(x^2+y^2)] \tag{1}$$

which is convolved with the image. This results in circular features appearing brighter than in the original image and so these can now be extracted by labelling all bright connected components within the image. Suppose k features are extracted. Each feature or putative pore $i \in \{1,\ldots,k\}$ is a connected set of pixels Λ_i and its location is determined as the centroid $\vec{c}_i$ given by

$$\vec{c}_i = \frac{\sum_{(x,y)\in\Lambda_i}(x,y)f(x,y)}{\sum_{(x,y)\in\Lambda_i} f(x,y)}.$$

Here $f(x,y)$ denotes the grey level value of the filtered image at pixel (x,y). Furthermore, a local, Hanning window w of size $n \times n$ is centred at each feature i and the vector $\boldsymbol{v}_i$ comprising the weighted grey values of the pixels in w is recorded.

Next, a model for the grey-level distribution in the local window w around a pore centre is estimated based on a PCA on a subset of extracted putative pores. In order to restrict estimation to features that are indeed pores we only consider pores whose size of associated pixel set Λ_i is below a given threshold. Let $\mathcal{S}$ be the index subset of the features selected. A PCA was then applied to the vectors $\boldsymbol{v}_i, i \in \mathcal{S}$, yielding a mean μ and eigenvectors $\gamma_1,\ldots,\gamma_n$.

Finally, each feature $i \in \{1,\ldots,k\}$ is considered for inclusion in the final set of pores. For each feature we compute the normalised residual error ϵ_i

given as

$$\epsilon_i = \|\boldsymbol{v}_i - \alpha_i \boldsymbol{\mu} - \sum_{j=1}^{m} \beta_{ij} \boldsymbol{\gamma}_j\|^2 \|\boldsymbol{v}_i\|^{-2}$$

where the coefficients α_i, β_{ij} are chosen to minimise the error. Feature i is then classified as a pore if ϵ_i is below a chosen threshold. All thresholds were chosen empirically to minimize the error rate, based on a sample print which had been annotated by an expert.

Appendix B The spatial summary statistics

In the following we give a more formal definition of the summary statistics used in this paper. More details can be found in [5].

Suppose we compare realisations of two point processes in a sampling window W. Let $\mathbf{1}_{[A]}$ denote the indicator function, that is

$$\mathbf{1}_{[A]} \quad = \quad \begin{cases} 1 & \text{if } A \text{ is true} \\ 0 & \text{otherwise} \end{cases}$$

Assume we observe n events in the first realisation and let y_i denote the distance from event i in the first realisation to its nearest event in the second realisation. Then the distribution of the distance between a typical event in the first point process and its nearest event in the second point process is denoted as G_{12}. An (edge-corrected) estimator of G_{12} is given by

$$\hat{G}_{12}(y) \quad = \quad \frac{\sum_{i=1}^{n} \mathbf{1}_{[y_i \le y,\, d_i > y]}}{\sum_{i=1}^{n} \mathbf{1}_{[d_i > y]}}$$

where d_i denotes the distance of the event i from the boundary of W.

For a stationary point process the mean number λ of points per unit area is called the intensity and can be estimated as $\widehat{\lambda} = \frac{n}{|W|}$. If we were to compare two independent realisation from a stationary Poisson process of intensity λ, then the distribution function G_{12} would be equal to the empty-space function F_2. For a stationary point process, the empty space function F_2 is the distribution function of the distance between an arbitrary point in the sampling window W to the nearest event. For a Poisson process of intensity λ it is given by

$$F_2(y) \quad = \quad 1 - \exp(-\lambda \pi y^2).$$

and can be estimated as

$$\widehat{F}_2(y) \quad = \quad 1 - \exp(-\widehat{\lambda} \pi y^2)$$

The univariate K-function of a point pattern is defined as

$$\lambda K(t) = \mathbb{E}(N(t))$$

where $N(t)$ is the number of further events within distance t of a typical event. The theoretical K-function of a Poisson process is given by $K(t) = \pi t^2$ and an edge-corrected estimator for K is given by

$$\hat{K}(t) = \frac{|W|}{n(n-1)} \sum_{i=1}^{n} \sum_{j \neq i} \frac{\mathbf{1}_{[u_{ij} \leq t]}}{w(x_i, u_{ij})}.$$

Here n is the total number of events, u_{ij} is the distance between the ith and the jth event and $w(x_i, u_{ij})$ is the circumference of a circle with centre x_i and radius u_{ij} that lies within W.

The above statistic can be extended to the bi-variate case. Explicitly then let

$$\lambda_2 K_{12}(t) = \mathbb{E}(N_{12}(t))$$

where λ_2 is the intensity of pattern 2 and $N_{12}(t)$ the number of events in pattern 2 within distance t of a typical event in pattern 1. An edge-corrected estimator for $K_{12}(t)$ is defined as follows. Let

$$\tilde{K}_{12}(s) \quad = \quad \frac{|W|}{n_1 n_2} \sum_{i=1}^{n_1} \sum_{j=1}^{n_2} w(x_i, u_{ij})^{-1} \mathbf{1}_{[u_{ij} \leq s]}.$$

Here n_1 is the number of points in pattern 1, n_2 the number of points in pattern 2 and u_{ij} is the distance between the ith point in pattern 1 and the jth point in pattern 2. As before, $w(x_i, u_{ij})$ is the circumference of a circle with centre x_i and radius u_{ij} that lies within W.

Acknowledgements: We thank Dr Roberto Puch Solis from the UK Forensic Science Service and Helen Bandey from the UK Police Science Development Branch for their support during this study and provision of data.

References

[1] D.R. Ashbaugh, "Poroscopy", *RCMP Gazette,* 45, 12-17, 1983.

[2] C. Champod, Fingerprints (Dactyloscopy): "Standard of Proof" in *Encyclopedia of Forensic Science* ed. G. Knupfer, Academic Press, London, 884 - 890. 2000.

[3] C. Champod, C.J. Lennard, P.A. Margot and M. Stoilovic, *"Fingerprints and other ridge skin impressions"*, Taylor and Francis Publishing, Boca Raton. 2004.

[4] C. Champod and P.A. Margot, "Analysis of Minutiae Occurrences in Fingerprints - The search for Non-Combined Minutiae". In *Current topics in Forensic Science" - Proceedings of the 14th Meeting of the International Association of Forensic Sciences*, Shundersons Communications, Ottowa, 55-58. 1997.

[5] P.J.Diggle, *"Statistical Analysis of Spatial Point processes"* Arnold, London, 2003.

[6] T.-I.Hsu and R.G. Wilson, "A two-component model of texture for analysis and synthesis" *IEEE Transactions in Image Processing*, 4(10):1466-1476, 1998.

[7] D. Maltoni, D. Maio, A.K. Jain and S. Prahabkar, *Handbook of Fingerprint Recognition*, Berlin, Springer-Verlag, 2003.

[8] W.J.Krzanowski, *Principles of Multivariate Analysis: A User's perspective*. Oxford Press, Oxford. 1988.

[9] D. Marr, *"Vision"*, San Francisco, Freeman, 1982.

[10] A. Jain, Y. Chen and M. Demirkus, "Pores and Ridges: Fingerprint Matching Using Level 3 Features", *ICPR 2006*. 18th International Conference on Pattern Recognition, 4:477-480, 2006.

[11] R Development Core Team *"R: A Language and Environment for Statistical Computing"* R Foundation for Statistical Computing, Vienna, Austria. 2004. ISBN 3-900051-07-0, URL http://www.R-project.org

[12] A. Roddy and J.D. Stosz, "Fingerprint features - Statistical analysis and system performance estimates", *Proceedings of the IEEE*, 85(9):1389-1421, 1999.

[13] A. Roddy and J.D. Stosz, "Fingerprint Feature Processing Techniques and Poroscopy"˙ In *Intelligent Biometric Techniques in Fingerprint and Face Recognition*, ed L.C. Jain, U. Halici, I. Hayashi and S.B. Lee, CRC Press, Boca Raton, 37 -105, 1995.

[14] J.D. Stosz and L.A. Alyea, "Automated system for fingerprint authentication using pores and ridge structure" *Proceedings of SPIE, Automatic*

Systems for the Identification and Inspection of Humans, 2277, 210-223, 1994.